Origin of the *n*-type and *p*-type conductivity of MoS$_2$ monolayers on a SiO$_2$ substrate

Kapildeb Dolui, Ivan Rungger, and Stefano Sanvito

School of Physics and CRANN, Trinity College, Dublin 2, Ireland
(Received 11 January 2013; published 2 April 2013)

Ab initio density functional theory calculations are performed to study the electronic properties of a MoS$_2$ monolayer deposited over a SiO$_2$ substrate in the presence of interface impurities and defects. When MoS$_2$ is placed on a defect-free substrate, the oxide plays an insignificant role since the conduction band top and the valence band minimum of MoS$_2$ are located approximately in the middle of the SiO$_2$ band gap. However, if Na impurities and O dangling bonds are introduced at the SiO$_2$ surface, these lead to localized states, which modulate the conductivity of the MoS$_2$ monolayer from *n*- to *p*-type. Our results show that the conductive properties of MoS$_2$ deposited on SiO$_2$ are mainly determined by the detailed structure of the MoS$_2$/SiO$_2$ interface, and suggest that doping the substrate can represent a viable strategy for engineering MoS$_2$-based devices.

I. INTRODUCTION

Recently, MoS$_2$-based layered transition-metal dichalcogenides (LTMDs) have attracted considerable attention due to their potential for constructing low-dimensional nanostructures for a variety of applications.[1–3] The electronic properties of MoS$_2$ show a strong dependence on thickness,[4] i.e., on the number of atomic layers forming a given sample. In particular, MoS$_2$ monolayers, which display a substantial direct band gap, represent a semiconducting alternative to graphene, which is a metal in its pristine form. Although the band gap of graphene can be opened by fabricating nanoribbons[5] or by depositing it on a suitable substrate,[6] this comes to the prize of deteriorating, in a somehow uncontrollable way, the carrier mobility due to edges and impurity scattering.[7] In contrast, the low dimensionality, the small amount of dangling bonds, and their typical high crystalline form, make the performances of LTMD-based transistors comparable to those of existing Si-based ones.[8–10] In particular, transistors made from MoS$_2$ monolayers have been recently fabricated, showing a mobility of at least 200 cm^2/V s at room temperature, an on/off current ratio of 10^8, and low standby power dissipation.[14]

Although the MoS$_2$ bulk conductivity is often mentioned to show *n*-type character,[11–13] both *n*-type[14–17] and *p*-type[18,19] conductivities have been reported in ultrathin MoS$_2$ layers deposited on SiO$_2$. The conducting behavior of MoS$_2$ therefore seems to depend on the experimental details and an explanation for the specific current polarity (*n*- or *p*-type) remains far from being clear. Note that no intentional doping was introduced in the experiments mentioned above, so that the source of the different carrier types should be intrinsic to the MoS$_2$ layer, to the substrate, and to the interaction between the two.

The possible creation of Mo and/or S vacancies during the growth can not be the cause of the various conductive properties since vacancies create deep levels at midgap in the band structure of MoS$_2$ monolayers.[20] Notably, disorder at the semiconductor/substrate interface in general plays a crucial role in determining the conductive properties of ultrathin devices. For example, for GaAs nanowires, it has been demonstrated that upon decreasing the nanowire diameter, the interface-mediated conductivity gradually becomes dominant over the bulk one.[21] Such surface sensitivity can also be used to one's advantage. For instance, an ambipolar transistor has been

realized in MoS$_2$ thin flakes by contact with an ionic liquid environment,[13] which as well affects the interface properties. Since MoS$_2$ monolayers are placed on insulators in practically any device architecture, it is important to identify the possible effects that the substrate has on the conductivity. Note that during the synthesis and the sample preparation, SiO$_2$ can adsorb relatively light impurities, such as Na and K,[22] on its surface.

The position of the Fermi energy of two-dimensional (2D) materials with respect to their valence and conduction bands depends on the Fermi energy of the surroundings, and especially interfacial defects can play a significant role. The defects responsible for the conductive properties of low-dimensional devices are expected to be extrinsic in nature, such as charged impurities at the interface between the conductive channel and the substrate. These lead to an inhomogeneous Coulomb potential for both conduction and valence band electrons. Such charge traps have been identified to be in the form of adsorbates or defects at the surface of the underlying substrate in the case of graphene.[23,24] Likewise, temperature-dependent transport measurements on thin MoS$_2$ layers, down to the monolayer limit, suggest that trapped charges at the SiO$_2$ surface could be responsible for the observed *n*-type behavior, when MoS$_2$ is deposited on SiO$_2$.[25]

In general, when charged traps are located at an interface, they influence the depletion/accumulation of electrons in the conducting channel up to a certain thickness, which is proportional to the channel screening length. This distance depends on different physical features, such as the nature and the density of the traps, and the electronic properties of the channel. For conventional semiconductors, it typically reaches up to a few nanometers. For instance, it has been recently demonstrated that charged trap states at the substrate/channel interface significantly affect the conductivity of GaAs nanowires up to diameters of about 40–70 nm.[21] More dramatic effects are expected for layered compounds down to the single-layer limit, in which essentially all the atoms are at the interface with the substrate and the channel vertical dimension is certainly shorter than the screening length. Recently, a reduction in conductivity with increasing the MoS$_2$ film thickness has been observed in MoS$_2$-based transistors, where SiO$_2$ was used as back gate.[26] This suggests that for

the MoS_2/SiO_2 system, the transport is interface mediated, as intrinsic defects, homogeneously distributed in MoS_2, would not lead to any dependence of the conductivity on thickness.

In order to shed some light on the effects that trap states at the SiO_2 surface have on the conductive properties of MoS_2/SiO_2 hybrid systems, we have performed state-of-the-art first-principles electronic-structure calculations. In particular we have considered the case when the traps are due to impurities such as immobile Na and H atoms, and O-dangling bonds. The paper is organized as follows. In the next section we briefly describe our computational techniques and we provide details of the simulations performed. Then we proceed with presenting the results of this work in the context of recent experiments, and finally we conclude.

II. METHODOLOGY

In order to investigate the influence of a SiO_2 substrate on the electronic properties of a MoS_2 monolayer, *ab initio* calculations are performed by using density functional theory[27,28] (DFT) within the generalized gradient approximation (GGA) of the exchange and correlation (XC) functional as introduced by Perdew, Burke, and Ernzerhof[29] (PBE) and numerically implemented in the SIESTA code.[30] In our calculations, a double-ζ polarized[31] numerical atomic orbital basis set is used for all the atoms, and the basis set is constructed using the default SIESTA value for the energy shift (0.01 Ry). The Troullier-Martins scheme is employed for constructing the norm-conserving relativistic pseudopotentials[32] (no semicore states are included in the pseudopotential generation). An equivalent plane-wave cutoff of 350 Ry is chosen in all the simulations and the Brillouin zone is sampled by using an equivalent k-grid cutoff of 17 Å. Relaxed geometries are obtained with the conjugate gradient method, where all the atoms in the supercell are allowed to relax until the force on each atom is less than 0.02 eV/Å. Note that we do not fix the atoms of the bottom layers during relaxation.

A trap state is usually formed when an energy level associated either to a defect or an impurity appears within the energy gap of the host material. Such trap states influence the charge transport properties mainly in two ways. First, if the traps are charged, they will capture a hole or an electron from the environment. This produces a modification of the electrostatic potential, which in turn shifts the level alignments in the system, and thus affects the conductivity. Second, they can also increase the carrier concentration and provide pathways for electrons or holes to hop. The efficiency of this process depends on the amount of localization of the states associated to the defect site. If the energy of the localized gap state is close to either the valence band maximum (VBM) or the conduction band minimum (CBM), then at a given temperature some of these charges will be transferred either to the conduction or to the valence band, where they may contribute to increase the system conductivity.

Whether or not one can describe with *ab initio* calculations such mechanisms depends crucially on the ability of computing accurately the energy levels of the system. The use of the GGA [or of the local density approximation (LDA)] for electronic-structure calculations of defect levels is, in general, problematic. One reason is the typical underestimation of the energy gap and the related incorrect alignment of the energy levels of hybrid systems. For instance, an artificially reduced band gap may erroneously bring deep traps in resonance with either the conduction or the valence band.[33,34] A second source of error is the incorrect description of the charge localization at the defect site, a feature that usually leads to predict defects to be too shallow.[35] Atomic self-interaction correction[36,37] (ASIC) has been proved to overcome these deficiencies.[38,39] Therefore, we also perform additional LDA + ASIC calculations to verify the robustness of the LDA/GGA results. In particular, we set the ASIC scaling parameter to $\alpha = 0.5$, a value which is generally appropriate to mid-gap insulators.[36]

III. RESULTS AND DISCUSSION

A. Defect-free SiO_2 interface

Substantial experimental efforts have been devoted to deposit ultrathin MoS_2 layers onto SiO_2 in order to demonstrate transistor operation, down to the single-layer limit.[14,15,19] Usually amorphous oxides are used as substrates. However, in order to avoid the computational complexity of a highly disordered structure, a crystalline SiO_2 substrate is simulated here instead. This also allows us to systematically determine the effects of individual defects and impurities on the electronic structure of a MoS_2 layer. Our unit cell is constructed as a slab containing eight Si atomic layers for siloxane, and six Si atomic layers for silanol, with the structure of α quartz, and an adsorbed MoS_2 monolayer. At least 15 Å of vacuum are included at the slab boundaries to avoid the spurious interaction between the slab periodic images. We consider the modified oxygen-terminated SiO_2 (0001) surface in order to simulate the most experimentally relevant conditions.

Two primary structures for the oxygen-terminated SiO_2 (0001) surface are possible, depending on whether the termination is with the siloxane group (Si-O-Si) or with the silanol one (Si-OH). Both surfaces can form depending on the surface treatment.[40] The siloxane reconstruction at room temperature forms an O-terminated surface with an outermost six-membered ring structure, as shown in Figs. 1(a) and 1(b). Under annealing in ambient conditions, it becomes hydroxylated (Si-OH) and the reconstruction transforms into the silanol one, which presents on the surface a zigzag H-bonded network [see Figs. 1(c) and 1(d)]. In both cases, in our simulations the dangling bonds on the Si-terminated bottom surface are saturated by hydrogen.

The optimized lattice constants of the pristine SiO_2 and MoS_2 are 4.91 and 3.19 Å, respectively. We therefore construct a hexagonal supercell in the plane, with a 9.69-Å-long side, so that the lattice mismatch between SiO_2 and MoS_2 is minimized to ~1.2 %. The GGA calculated band gap of SiO_2 and of a MoS_2 monolayer are 6.20 and 1.49 eV, respectively. The small strain applied to the MoS_2 monolayer changes only little the electronic structure. The band gap remains direct at the K point and it is only reduced by 0.22 eV from the value of 1.71 eV obtained for the unstrained case. We expect that the small strain will only lead to minor quantitative changes of the results. Similarly to the case of graphene,[41] we expect that the electronic structure of a defect-free MoS_2 monolayer is only marginally affected by its local arrangement on the
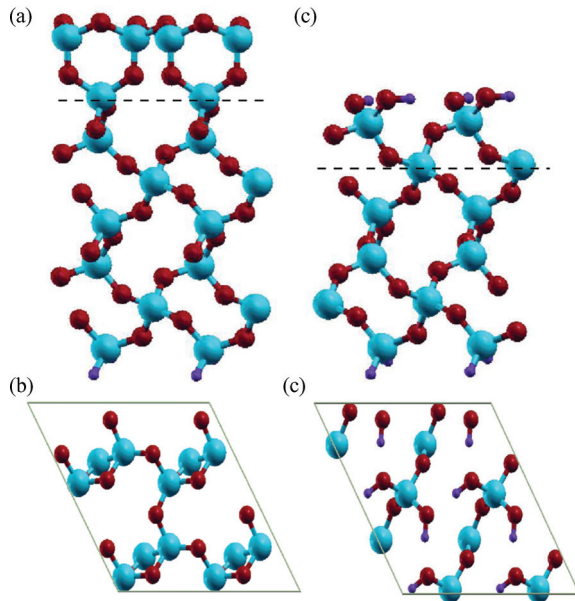
FIG. 1. (Color online) Side and top views of reconstructed structures for the O-terminated SiO_2 (0001) (siloxane) surface [(a) and (b)], and the fully hydroxylated SiO_2 (0001) (silanol) one [(c) and (d)] (color code: cyan $\rightarrow$ Si, red $\rightarrow$ O, violet $\rightarrow$ H). For clarity, only the top layers of SiO_2 (above the dashed line) are shown in the top views.

pristine SiO_2 substrate. Therefore, as a representative configuration, we use the arrangement of Fig. 2, where an oxygen atom is situated at the hollow site of the Mo surface triangles.

We start our discussion by presenting the properties of the defect-free hybrid MoS_2/SiO_2 system. The equilibrium distances d_0 between the SiO_2 and the MoS_2 surfaces are 3.01 and 2.98 Å for siloxane and silanol, respectively. Here, d_0 is defined as the vertical separation between the topmost O layer in the SiO_2 surface and its nearest S layer in MoS_2. These values are similar to the distance between two MoS_2 monolayers that we calculate to be 3.17 Å. Note that in general GGA-type XC functionals do not describe accurately van der Waals forces. It has been shown that the GGA exchange-correlation functional usually overestimates the interlayer spacing[42] and underestimates the binding energy of layered dichalcogenides.[43] However, for bulk MoS_2, we find that our calculated interlayer binding energy of 17 meV/Å^2 is in rather good agreement with the value of 20.53 meV/Å^2 obtained by using the random phase approximation for the electronic correlation.[43] The binding energy of the MoS_2/SiO_2
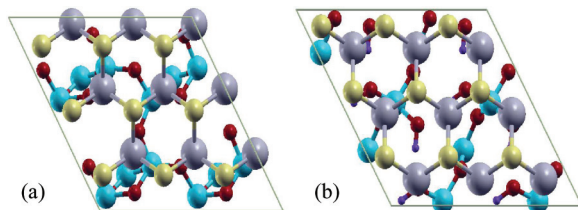

FIG. 2. (Color online) Top view of the optimized structure of MoS_2 placed on a defect-free (a) siloxane and (b) silanol surface (color code: light gray $\rightarrow$ Mo, yellow $\rightarrow$ S, cyan $\rightarrow$ Si, red $\rightarrow$ O, violet $\rightarrow$ H). Only the top layers of SiO_2 are shown (see Fig. 1).

system is given by $E_b = E_{MoS_2} + E_{SiO_2} - E_{MoS_2/SiO_2}$, where E_{MoS_2}, E_{SiO_2}, and E_{MoS_2/SiO_2} are total energies of the isolated MoS_2, the isolated SiO_2 slab, and of the MoS_2/SiO_2 hybrid system, respectively. We find E_b for siloxane and silanol to be, respectively, 13 and 15 meV/Å^2. These binding energies are close to that between two MoS_2 layers (19 meV/Å^2), which are bound together by the rather weak van der Waals forces. As such, our results show that MoS_2 is weakly bound also to the SiO_2 surface, in agreement with recent experimental results that have measured the interaction between MoS_2 and an underlying SiO_2 substrate to be negligible.[44]

We have then verified that our calculated d_0 for bulk MoS_2, $d_0 = 3.08$ Å, is in good agreement with the experimental value of 2.96 Å (Ref. [45]) and also with the previously calculated theoretical estimate of 3.05 Å.[46] Moreover, in order to take into account possible small deviations of the relaxed distance from the experimental value due to the XC functional used, we have evaluated the electronic structure for d_0 within the range $d_0 \pm 0.5$ Å, and we have found that the results change little with varying the distance.

B. SiO_2/MoS_2 composite with siloxane reconstruction

We now move to study the electronic structure of a MoS_2 monolayer deposited on SiO_2 by starting with the siloxane surface. In particular, we consider first the situation where SiO_2 is defect free. Figure 3(c) shows the density of states (DOS) of the hybrid SiO_2/MoS_2 system, which remains semiconducting with a band gap of 1.48 eV, i.e., with the same band gap of a freestanding MoS_2 monolayer having the same lattice parameters. Both the valence and the conduction bands of the hybrid compound are associated to MoS_2. We note that the projected DOS (PDOS) over MoS_2 extends into the SiO_2 band gap, and the total DOS of the combined material is essentially given by the superposition of the DOSs of the pristine slab of SiO_2 [Fig. 3(a)] and of the MoS_2 monolayer [Fig. 3(b)]. The conduction and the valence bands of SiO_2 are located respectively at 2.1 and 2.6 eV away from those of MoS_2. As a consequence, no charge transfer between the substrate and MoS_2 occurs. Importantly, one of the basic criteria for the selection of the gate oxide is fulfilled here, namely, that the oxide should have a band offset of over 1 eV for both the conduction and valence bands in order to create a large barrier for both electrons and holes.[47] Our results show that the conductivity of MoS_2 is not influenced by the underlying defect-free SiO_2 substrate. Therefore, the measured *n*- or *p*-type conducting properties of MoS_2 on SiO_2 must be due to defects and impurities.

Localized states, arising from impurities or defects within the oxide substrate or at the interface with the conducting channel, can redefine the effective Fermi level of the hybrid system, as illustrated schematically in Fig. 4. Depending on the alignment of the gap states with respect to the MoS_2 valence and conduction bands, the system can switch from *n*-type [see Fig. 4(b)] to *p*-type [see Fig. 4(c)]. Therefore, such trap states are expected to give significant contributions to the conductivity of these low-dimensional systems. In the layered structure considered in this work, the trap states are expected to be located at the interface between the LTMDs and the substrate, not in the LTMDs themselves, which usually are
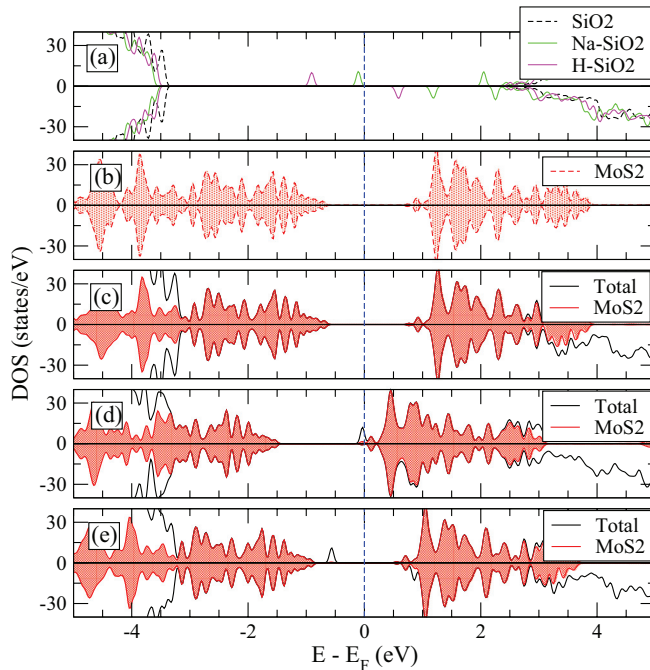
FIG. 3. (Color online) Electronic structure of the SiO_2/MoS_2 hybrid system when various defects are present at the SiO_2 siloxane surface. (a) The total DOS for the defect-free surface (black, dashed curves), and when either Na (green, solid curves), or H adsorbed (magenta, solid curves) are adsorbed. (b) The DOS of a pristine freestanding MoS_2 monolayer. The total DOS and the PDOS for MoS_2, when the MoS_2 monolayer is placed on the defect-free siloxane surface (c), on a siloxane surface with one adsorbed Na (d), or with one adsorbed H (e). The blue dashed vertical line indicates the Fermi level, which has been set to zero in all the panels. The red shaded areas indicate the MoS_2 PDOS. Positive and negative DOS are respectively for spin-up (majority spins) and spin-down (minority spins) electrons.

highly defect free. Trap states at the SiO_2 surface can have a wide range of origins, such as immobile ionic charges, SiO_2 surface dangling bonds, and foreign impurities adsorbed on the surface.[48] In literature, densities of trap states on SiO_2 are reported in the range[49] 10^{10}–10^{14} cm^{-2}. As representative dopants, here we consider two possible candidates: Na atoms and SiO_2 surface oxygen dangling bonds.

In order to simulate the effects of such impurities on the electronic structure of the MoS_2 channel, a single Na atom is placed on top of the siloxane SiO_2 surface. Given the lateral dimension of our supercell, this corresponds to an impurity density of $\sim 10^{14}$ cm^{-2}, which is close enough to the recently reported values of trap state densities, reaching up to $\sim 10^{13}$ cm^{-2} for thin MoS_2 layers deposited on SiO_2.[8,26] The most energetically favorable binding position for Na is found to be at the center of the surface oxygen triangle [see Fig. 5(a)]. A Na adatom adsorbed on a pristine SiO_2 surface creates a deep donor state in the DOS, with a single-particle level at about 2 eV below the SiO_2 CBM [see Fig. 3(a)]. Note that such state is singly occupied and therefore spin splits in our spin-polarized calculations, with the empty minority spin state (spin down) laying approximately 1 eV below the CBM and 1 eV below the Fermi level.
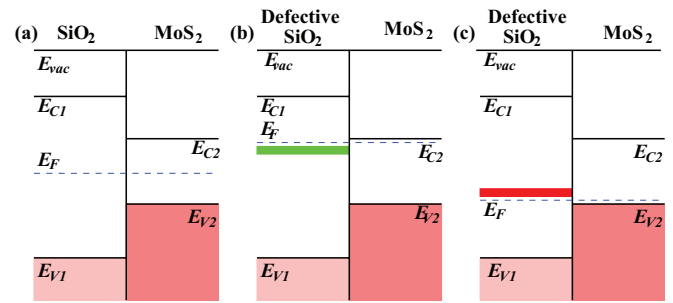

FIG. 4. (Color online) Schematic band diagram for MoS_2 placed on the defect SiO_2 substrate (a), and on a substrate including a defect-induced donor (b) or acceptor (c) level. This demonstrates the modulation of the conductivity from n- to p-type as the impurity state redefines the Fermi energy in the oxide. The energy levels E_V, E_C, E_F, and E_{vac} define the valence band maximum (VBM), the conduction band minimum (CBM), the Fermi energy, and the vacuum level, respectively. The subscripts 1 and 2 refer to SiO_2 and MoS_2, respectively. The blue dashed lines indicate the Fermi energy of the hybrid system (common to SiO_2 and MoS_2). The thick green line in (b) indicates the donor level and the thick red line in (c) represents the acceptor state in the oxide. Note that in general due to charge transfer from MoS_2 to the gap states, and the related dipole formation, the level alignment between E_{V1} and E_{V2} will also change in the defective systems.

When a MoS_2 monolayer is deposited over the Na-doped SiO_2 surface, d_0 increases to 3.24 Å at the edges of our unit cell, whereas at the Na site the O-S distance becomes 3.45 Å. The enlargement of the binding distance compared to that of the pristine SiO_2/MoS_2 system is a direct consequence of the Na intercalation at the interface. The electronic structure of the composite is strongly affected by the presence of the Na ion, as shown in Fig. 3(d). Also, in this case the total DOS appears as a direct superposition of those of SiO_2 and MoS_2. However, the presence of the Na-filled state shifts the Fermi level, which now gets pinned just below the MoS_2 CBM. The resulting DOS around E_F is thus that of the defect-free MoS_2 conduction band with the addition of a Na-derived impurity level positioned below it. Hence, the gap state is moved below the Fermi energy, resulting in a very small activation energy for the transfer of electrons from Na to the MoS_2 conduction
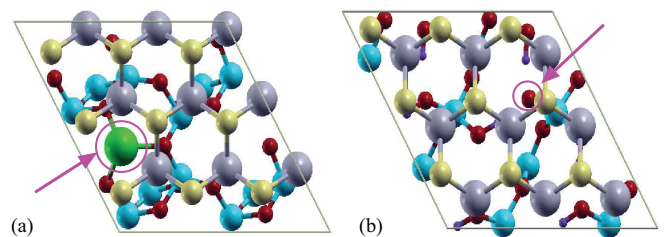

FIG. 5. (Color online) The optimized geometry for MoS_2 placed on (a) the siloxane surface incorporating a Na impurity and (b) the dangling oxygen bond on the silanol surface, obtained by removing a H atom. The arrows indicate the positions of the defects on the surface (color code: green $\rightarrow$ Na, while the other colors are the same atoms as in Fig. 2). The arrows indicate the location of the impurities/defects. Only the top layers of SiO_2 are shown (see Fig. 1).

band. This is the situation schematically presented in Fig. 4(b), which leads to *n*-type doping.

If we now replace Na with H on the SiO$_2$ siloxane surface, the associated filled gap state lies deep in the SiO$_2$ band gap [see Fig. 3(a)], despite the fact that H and Na share the same *s*-like valence. The same situation persists in the composite [see Fig. 3(e)], where the H-derived filled spin-up level remains at mid-gap, approximately 0.5 eV above the VBM, while the empty spin-down one is nearly resonant within the conduction band. This situation, however, does now lead to doping so that H can not influence the conductivity of the MoS$_2$/SiO$_2$ structure. The quantitative difference found between the results for the Na and the H cases show that, in order to obtain *n*-type character, only impurities with rather small ionization potential are relevant. These can transfer one electron to the MoS$_2$ conduction band with small activation energy. Such activation energy is a key factor in the determination of the threshold voltage V_{th}, required to operate a transistor in the on state. As a consequence, the experimentally measured values for V_{th}, which show a large variation for different samples,[25] are then attributable to varying concentrations and properties of the trap states from sample to sample. We note that, although for the perfectly crystalline substrate the defect state is deep in the gap, for disordered substrates local potential fluctuations may shift the energy levels of individual defects towards the conduction band. Moreover, a change of the position of MoS$_2$ with respect to the SiO$_2$ substrate might also lead to a change of the exact energy of the defect states.

C. SiO$_2$/MoS$_2$ composite with silanol reconstruction

Next, we move to examine the case of the SiO$_2$ surface with silanol reconstruction, the DOS of which is presented in Fig. 6(a). Similarly to the siloxane case, the PDOS for the defect-free MoS$_2$/SiO$_2$ composite [see Fig. 1(b)] corresponds to a superposition of the DOSs of the isolated MoS$_2$ [Fig. 3(b)] and SiO$_2$ [Fig. 6(a)] components, indicating weak interaction between the two materials. When a Na atom is intercalated between the silanol surface and the MoS$_2$ layer, we find that the system becomes *n*-type [Fig. 6(c)], in the same way as for the siloxane surface. This indicates that Na is an efficient *n* dopant for MoS$_2$ on SiO$_2$ regardless of the surface reconstruction.

In general, thermal annealing of the silanol surface creates undercoordinated oxygen atoms (Si-O*). These appear as stable surface defect centers and act as typical charge traps in oxygen-rich SiO$_2$ (Ref. 50) since they are able to capture an extra electron in their dangling bond. In our calculations, such defects are created on the Si-OH surface by removing a H atom from the top surface [see Fig. 5(b)]. For such a defect we find that the empty acceptor state is created ∼0.9 eV above the SiO$_2$ VBM [see Fig. 6(a)]. Once MoS$_2$ is layered onto the surface, the value of d_0 at the boundary of our H-deficient unit cell is $d_0 = 2.98$ Å, which is approximately equal to that for the pristine surface, whereas at the dangling bond site the O-S distance is significantly reduced to 2.68 Å. When placing the MoS$_2$ monolayer on this defective surface, the dangling bond state gets filled by capturing an electron from the MoS$_2$ valence band, so that the Fermi energy now lies just below the MoS$_2$ VBM [see Fig. 6(d)]. This is the level alignment presented in Fig. 4(c), which makes the composite *p*-type. Note that the
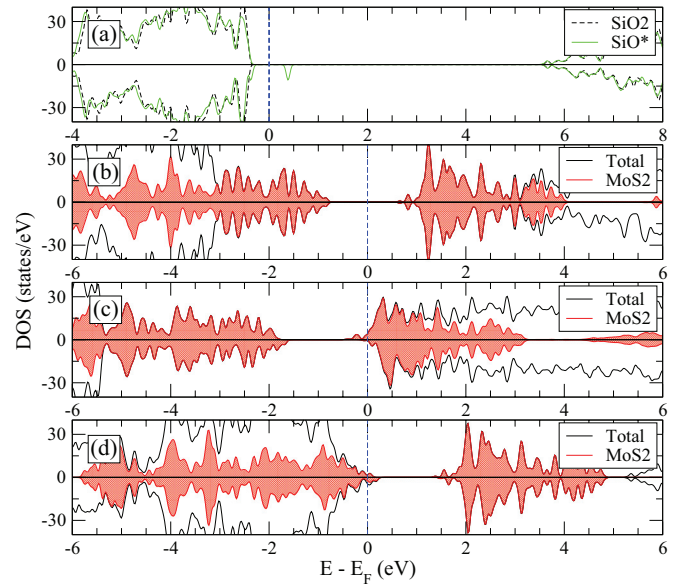

FIG. 6. (Color online) Electronic structure of the SiO$_2$/MoS$_2$ hybrid system when various defects are present at the SiO$_2$ silanol-reconstructed surface. (a) The DOS for the defect-free surface (black, dashed curve) and for the one where one O dangling bond is induced by a single H removal (green, solid curve labeled as SiO*). The total DOS and the MoS$_2$ PDOS for the SiO$_2$/MoS$_2$ composite when the MoS$_2$ monolayer is placed on (b) the defect-free surface, (c) on the surface with a single adsorbed Na atom, and (d) on the surface with an O dangling bond created by removing a single H atom. The blue dashed line indicates the Fermi energy, which is set to zero in all panels. The red shaded areas indicate the MoS$_2$ PDOS. Positive and negative DOS are, respectively, for spin-up (majority spins) and spin-down (minority spins) electrons.

rather high density of oxygen dangling bonds in our system causes a large surface charge density dipole, which shifts the MoS$_2$ DOS upwards in energy by more than 1 eV with respect to the SiO$_2$ substrate. By modulating the density of such defect types, one may be able to change such a shift.

D. Robustness of the results against the choice of XC functional: ASIC

Finally, in order to verify that the calculated level alignment is robust against the choice of exchange and correlation functional, we have repeated our calculations by using the ASIC scheme. As expected, the ASIC functional increases the band gap of MoS$_2$ and SiO$_2$, respectively, to 1.73 and 8.02 eV (for the same strained hybrid structure used in the previous sections). In the case of SiO$_2$, this brings the calculated value sensibly closer to the experimental one of 8.9 eV,[51] as expected from the ASIC when dealing with an insulator whose valence and conduction bands have different orbital content.[36,37]

The situation for MoS$_2$ is more complicated and deserves a detailed discussion. In this case, the band gap is defined by bands dominated mainly by Mo-*d* orbitals and the ASIC opens it only marginally. For a freestanding MoS$_2$ monolayer, the ASIC ($\alpha = 0.5$) returns a direct band gap of 2.03 eV (compared to a GGA gap of 1.71 eV). Note that the LDA value is 1.87 eV so that the LDA already partially opens the gap with respect to the GGA. It is also notable that an enhancement of
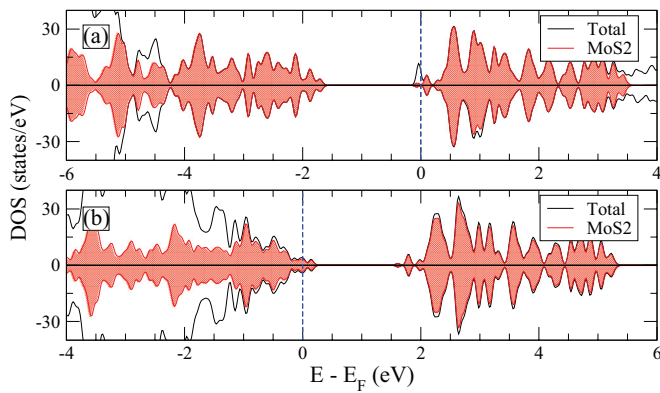
FIG. 7. (Color online) Density of states for the defective SiO_2/MoS_2 composite calculated with the ASIC XC functional. In panel (a), we report the DOS for the siloxane reconstruction with an intercalated Na atom [corresponding to Fig 3(d)], while in (b) that for the silanol reconstruction and an O dangling bond obtained by removing a surface H atom [corresponding to 6(d)].

the screening parameter α to $\alpha = 1$ (full atomic correction) produces a marginal further increase of the gap to 2.10 eV. Importantly, the ASIC result is rather close to that calculated[52] with the hybrid Heyd-Scuseria-Ernzerhof (HSE) exchange-correlation functional.[53] This is, however, larger than the optical band gap of 1.90 eV measured experimentally for MoS_2 monolayers.[15] The apparent contradiction can be solved by noting that the optical excitations involve excitons with a large binding energy of the order of 1 eV, as confirmed by many-body calculations.[52] Thus, one expects that the true quasiparticle spectrum has a band gap of approximately $1.9 + 1 = 2.9$ eV, in good agreement with that computed with the GW scheme, either at the first-order level[52] (2.82 eV) or self-consistently[54] (2.76 eV). As such, the ASIC describes MoS_2 with a band gap larger than the measured optical one and it provides an improved description over that of the GGA.

We now go back to the SiO_2/MoS_2 composite and in Fig. 7 we report two representative results for the case of Na adsorbed on the siloxane surface and for that of the O dangling bond on the silanol one. We find that for the first case, although the band gaps of the two parental materials are both increased, the Fermi energy is still pinned at the bottom of the MoS_2 conduction band [Fig. 7(a)]. As a consequence, Na still leads to an n-type semiconducting character with small activation barrier. Similarly, the O dangling bond on the silanol-terminated surface leads to a p-type semiconducting character [see Fig. 7(b)], with the Fermi energy positioned

below the MoS_2 valence band. This indicates that our two main results remain unchanged whether calculated at the GGA or ASIC level, i.e., they are robust with respect to the choice of exchange-correlation functional.

IV. CONCLUSION

The effects of the SiO_2 substrate on the conductivity of a semiconducting MoS_2 monolayer are investigated with first-principles density functional theory calculations. The defect-free SiO_2 surface does not affect significantly the electronic properties of MoS_2 due to their weak mutual interaction. As such, the conductive properties of MoS_2 do not change and SiO_2 appears as an ideal gate material. However, when Na atoms are placed at the SiO_2/MoS_2 interface, a shallow donor trap state is created just below the CBM of the hybrid SiO_2/MoS_2 composite. The small activation energy makes the hybrid MoS_2/Na-SiO_2 system an n-type semiconductor even for rather low temperatures. Interestingly, the behavior is different for H adsorption, where the impurity level is created ~ 0.9 eV below the CBM, resulting in a stable localized charge that can not be easily promoted to the CBM and does therefore not affect the conductivity.

In contrast, in the case of oxygen dangling bonds on the silanol-terminated SiO_2 surface, the Fermi energy of the MoS_2/SiO_2 system is located just below the VBM, making the system a p-type semiconductor. These results show that the conductivity of ultrathin semiconducting LTMDs changes from n- to p-type depending on the charge polarity of the traps, as well the energy-level alignment of the trap states within the LTMDs band gap. These kinds of trap states at the SiO_2 surface are likely to be at the origin of the observed change in conductance in different experimentally realized MoS_2-based transistors. Intriguingly, our results suggest the possibility of intentionally doping MoS_2 by depositing different adsorbates over the substrate SiO_2 surface. This can pave the way for a new strategy in the design of two-dimensional devices, where the electronic properties of the channel are engineered by manipulating those of the substrate.

[1]J. V. Lauritsen, J. Kibsgaard, S. Helveg, H. Topsøe, B. S. Clausen, E. Lægsgaard, and F. Besenbacher, Nat. Nanotechnol. **2**, 53 (2007).

[2]Z. Yin, H. Li, H. Li, L. Jiang, Y. Shi, Y. Sun, G. Lu, Q. Zhang, X. Chen, and H. Zhang, ACS Nano **6**, 74 (2012).

[3]Q. H. Wang, K. Kalantar-Zadeh, A. Kis, J. N. Coleman, and M. S. Strano, Nat. Nanotechnol. **7**, 699 (2012).

[4]A. Splendiani, L. Sun, Y. Zhang, T. Li, J. Kim, C.-Y. Chim, G. Galli, and F. Wang, Nano Lett. **10**, 1271 (2010).

[5]X. Wang, Y. Ouyang, X. Li, H. Wang, J. Guo, and H. Dai, Phys. Rev. Lett. **100**, 206803 (2008).

[6]S. Y. Zhou, G.-H. Gweon, A. V. Fedorov, P. N. First, W. A. de Heer, D.-H. Lee, F. Guinea, A. H. Castro Neto, and A. Lanzara, Nat. Mater. **6**, 770 (2007).

[7] S. Adam, E. H. Hwang, V. M. Galitski, and S. D. Sarma, Proc. Natl. Acad. Sci. USA **104**, 18392 (2007).

[8] A. Ayari, E. Cobas, O. Ogundadegbe, and M. S. Fuhrer, J. Appl. Phys. **101**, 014507 (2007).

[9] K.-K. Liu, W. Zhang, Y.-H. Lee, Y.-C. Lin, M.-T. Chang, C.-Y. Su, C.-S. Chang, H. Li, Y. Shi, H. Zhang, C.-S. Lai, and L.-J. Li, Nano Lett. **12**, 1538 (2012).

[10] L. Liu, S. B. Kumar, Y. Ouyang, and J. Guo, IEEE Trans. Electron Devices **58**, 3042 (2011).

[11] R. Fivaz and E. Mooser, Phys. Rev. **163**, 743 (1967).

[12] S. H. El-Mahblawy and B. L. Evan, Phys. Status Solidi B **79**, 713 (1977).

[13] Y. Zhang, J. Ye, Y. Matsuhashi, and Y. Iwasa, Nano Lett. **12**, 1136 (2012).

[14] B. Radisavljevic, A. Radenovic, J. Brivio, V. Giacometti, and A. Kis, Nat. Nanotechnol. **6**, 147 (2011).

[15] K. F. Mak, C. Lee, J. Hone, J. Shan, and T. F. Heinz, Phys. Rev. Lett. **105**, 136805 (2010).

[16] H. Li, G. Lu, Z. Yin, Q. He, H. Li, Q. Zhang, and H. Zhan, Small **8**, 682 (2012).

[17] Y.-H. Lee, X.-Q. Zhang, W. Zhang, M.-T. Chang, C.-T. Lin, K.-D. Chang, Y.-C. Yu, J. T.-W. Wang, C.-S. Chang, L.-J. Li, and T.-W. Lin, Adv. Mater. **24**, 2320 (2012).

[18] Z. Zeng, Z. Yin, X. Huang, H. Li, Q. He, G. Lu, F. Boey, and H. Zhang, Angew. Chem. Int. Ed. **50**, 11093 (2011).

[19] Y. Zhan, Z. Liu, S. Najmaei, P. M. Ajayan, and J. Lou, Small **8**, 966 (2012).

[20] C. Ataca and S. Ciraci, J. Phys. Chem. C **115**, 13303 (2011).

[21] N. Han, F. Wang, J. J. Hou, F. Xiu, S. Yip, A. T. Hui, T. Hung, and J. C. Ho, ACS Nano **6**, 4428 (2012).

[22] Horacio E. Bergna, *The Colloid Chemistry of Silica*, Advances in Chemistry, Vol. 234 (ACS, Washington, DC, 1994), Chap. 1, pp. 1–47.

[23] P. Joshi, H. E. Romero, A. T. Neal, V. K. Toutam, and S. A. Tadigadapa, J. Phys.: Condens. Matter **22**, 334214 (2010).

[24] T. O. Wehling, A. I. Lichtenstein, and I. Katsnelson, Appl. Phys. Lett. **93**, 202110 (2008).

[25] S. Ghatak, A. N. Pal, and A. Ghosh, ACS Nano **5**, 7707 (2011).

[26] H. Liu, J. Gu, and P. D. Ye, IEEE Electron Device Lett. **33**, 1273 (2012).

[27] P. Hohenberg and W. Kohn, Phys. Rev. **136**, B864 (1964).

[28] W. Kohn and L. J. Sham, Phys. Rev. **140**, A1133 (1965).

[29] J. P. Perdew, K. Burke, and M. Ernzerhof, Phys. Rev. Lett. **77**, 3865 (1996).

[30] J. M. Soler, E. Artacho, J. D. Gale, A. Gracía, J. Junquera, P. Ordejón, and D. Sánchez-Porta, J. Phys.: Condens. Matter **14**, 2745 (2002).

[31] J. Junquera, Óscar Paz, D. Sánchez-Portal, and E. Artacho, Phys. Rev. B **64**, 235111 (2001).

[32] N. Troullier and J. L. Martins, Phys. Rev. B **43**, 1993 (1991).

[33] S. Sanvito and C. D. Pemmaraju, Phys. Rev. Lett. **102**, 159701 (2009).

[34] A. Zunger, S. Lany, and H. Raebiger, Physics **3**, 53 (2010).

[35] A. Droghetti, C. D. Pemmaraju, and S. Sanvito, Phys. Rev. B **78**, 140404(R) (2008).

[36] C. D. Pemmaraju, T. Archer, D. Sánchez-Portal, and S. Sanvito, Phys. Rev. B **75**, 045101 (2007).

[37] A. Filippetti, C. D. Pemmaraju, S. Sanvito, P. Delugas, D. Puggioni, and V. Fiorentini, Phys. Rev. B **84**, 195127 (2011).

[38] A. Droghetti and S. Sanvito, Appl. Phys. Lett. **94**, 252505 (2009).

[39] C. D. Pemmaraju, R. Hanafin, T. Archer, H. B. Braun, and S. Sanvito, Phys. Rev. B **78**, 054428 (2008).

[40] K. Nagashio, T. Yamashita, T. Nishimura, K. Kita, and A. Toriumi, J. Appl. Phys. **110**, 024513 (2011).

[41] N. T. Cuong, M. Otani, and S. Okada, Phys. Rev. Lett. **106**, 106801 (2011).

[42] A. Kuc, N. Zibouche, and T. Heine, Phys. Rev. B **83**, 245213 (2011).

[43] T. Björkman, A. Gulans, A. V. Krasheninnikov, and R. M. Nieminen, Phys. Rev. Lett. **108**, 235502 (2012).

[44] S. W. Han, H. Kwon, S. K. Kim, S. Ryu, W. S. Yun, D. H. Kim, J. H. Hwang, J. S. Kang, J. Baik, H. J. Shin, and S. C. Hong, Phys. Rev. B **84**, 045409 (2011).

[45] J. A. Wollman and R. B. Somaono, Phys. Rev. B **13**, 3843 (1976).

[46] C. Ataca, M. Topsakal, E. Akturk, and S. Ciraci, J. Phys. Chem. C **115**, 16354 (2011).

[47] J. Robertson and B. Falabretti, J. Appl. Phys. **100**, 014111 (2006).

[48] Narain Arora, *Mosfet Modeling For VLSI Simulation* (World Scientific, Singapore, 2007), pp. 128 and 129.

[49] R. A. McKee, F. J. Walker, and M. F. Chisholm, Science **293**, 468 (2001); Y.-W. Tan, Y. Zhang, K. Bolotin, Y. Zhao, S. Adam, E. H. Hwang, S. DasSarma, H. L. Stormer, and P. Kim, Phys. Rev. Lett. **99**, 246803 (2007).

[50] M. Stapelbroek, D. L. Griscom, E. J. Friebele, and G. H. Sigel, J. Non-Crystalline Solids **32**, 313 (1979).

[51] B. El-Kareh, *Fundamentals of Semiconductor Processing Technologies* (Kluwer Academic, Norwell, MA, 1995).

[52] A. Ramasubramaniam, Phys. Rev. B **86**, 115409 (2012).

[53] J. Heyd, G. E. Scuseria, and M. Ernzerhof, J. Chem. Phys. **118**, 8207 (2003); **124**, 219906 (2006).

[54] T. Cheiwchanchamnangij and W. R. L. Lambrecht, Phys. Rev. B **85**, 205302 (2012).